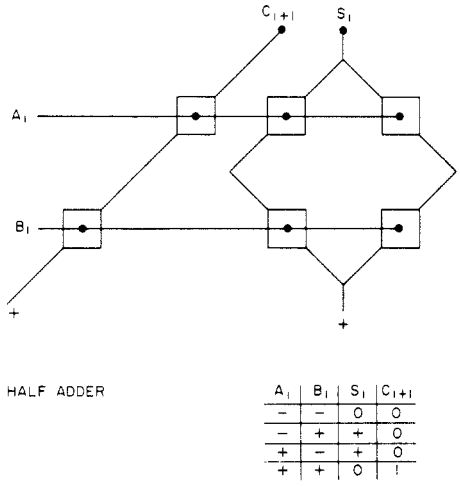

A_i	B_i	S_i	C_{i+1}
−	−	0	0
−	+	+	0
+	−	+	0
+	+	0	1

Figure 12. A molecular "HALF ADDER" for two input signals A_i and B_i and the added output C_{i+1}; S_i. The adder consists of the two logic gates "AND" and "EXCLUSIVE OR".

tetrathiafulvulenes on the other, some variations in the operation would result, such as nonlatching switches, which may have beneficial properties. These embodiments will be discussed in subsequent publications.

Conclusions

The spiro bridge that was proposed in this work is rather unique. It is capable of localizing an electron on one side of a molecule by providing a large tunneling barrier. On the other hand the same bridge is flexible toward electron transfer in electric fields, above threshold. Another important feature of the molecules studied is the exchange of the conductivity properties of the terminal groups. This interchange leads to possible device application in areas of signal processing on the molecular level.

The results of the dipole switching due to the action of the field above threshold and the simultaneous collapse of the tunneling barrier are complementary to each other. While the dipole reorientation emphasizes a static equilibrium outcome, the change from a double-well to a single-well molecule implies that the electron transfer will occur at a high rate, comparable at least to vibrational relaxations.

Our calculations show that the model proposed in this article does have the device properties that were presented. Actual implementation of some of the ideas outlined in this paper will be preceded by careful and laborious verifications, both theoretical and experimental, aimed at a deeper understanding of the basic principles involved. Clearly we need more profound knowledge of the through-bond vs through-space electron transfer and of the influence of electric fields on these types of mechanisms of electron transfer. Furthermore, practical molecules should be endowed with large polarizabilities in order to obtain switching with low fields. In short, we face a challenge and there is plenty to be done before we reap the technological benefits that might emerge.

The perceived novelty that the described model offers is the possible molecule-to-molecule communication that can lead to the synthesis of logic and amplification. One should not lose sight of the possible suitability of the proposed molecules for cellular automata. It is felt that the model could serve as a blueprint for molecular electronics.

Acknowledgment. I am pleased to acknowledge helpful discussions with Dr. Michel Dupuis, who supplied the latest version of HONDO and who had very useful suggestions for calculation of the overlap matrix. I am indebted to Dr. Angelo Rossi for installation of the HONDO program at the Watson Research Center and for advice on computational procedures. I also thank Dr. T. Schultz for an in-depth discussion of F. H. King's paper, Dr. C. Joachim for discussions on coupling in double-wells, and Professor M. A. Ratner for discussions on the problem of the overlap.

Experimental and Theoretical Study of Excimer Formation in 1-Azabicyclo[*l.m.n*]alkanes: Interpretation of Binding Energies Using a 3-Electron-Bond Model

Christopher J. Ruggles and Arthur M. Halpern*

Contribution from the Department of Chemistry, Northeastern University, Boston, Massachusetts 02115. *Received January 25, 1988*

Abstract: The excited dimer (excimer) of 1-azabicyclo[3.2.2]nonane (**322**) is reported. The binding energy is determined from a combination of transient and stationary photophysical measurements and found to be 22.2 kJ/mol in *n*-hexane solution. The binding energy of **322** is compared to those of other 1-azabicyclo[*l.m.n*]alkanes, **221** (51.0 kJ/mol) and **222** (36.8 kJ/mol). The observed changes are explained in terms of steric hindrance posed by the α-C hydrogen atoms, as excimer stability is achieved at close N–N approach. A theoretical model of an amine excimer, based on a neutral–radical cation pair, was used in conjunction with MNDO and AM1 calculations. Results of these calculations show that this type of 3-electron bonding is consistent with observed trends in the excimer stability. The failure of 1,4-diazabicyclo[2.2.2]octane (**DA222**) to manifest evidence of excimer formation, which is consistent with MNDO results, is rationalized in terms of the resonance stabilization of the **DA222** radical cation.

There has been long-standing interest in the structural dependence of molecular photoassociation.[1-3] Our particular concerns have centered on the photophysics and photoassociation of saturated amines in both the vapor and condensed phases. This paper is primarily concerned with three homologous compounds of the 1-aza bicyclic series (so-called "cage amines") and the excimers (*excited dimers*) of those species in alkane solution. Specifically, the amines examined are those for which [*l.m.n*] are **221**, **222**, or **322** and will be denoted as such throughout. In addition, experiments were performed on 1,4-diazabicyclo-[2.2.2]octane (**DA222**).

Interest in the structural effects on photoassociation arises for at least three reasons: (1) From the results of such studies, one can infer the consequences of similar structural features on any

(1) Halpern, A. M.; Legenza, M.; Ramachandran, B. R. *J. Am. Chem. Soc.* **1979**, *101*, 5736.
(2) Nosowitz, M.; Halpern, A. M. *J. Phys. Chem.* **1986**, *90*, 906.
(3) Halpern, A. M.; Ravinet, P.; Sternfels, R. J. *J. Am. Chem. Soc.* **1977**, *99*, 169.

0002-7863/88/1510-5692$01.50/0

reaction, regardless of the electronic states of the reactants. (2) One can determine differences in the reactivity of the electronically excited states of similar molecules. (3) Results shed light on the nature of the binding mechanism between excited- and ground-state molecules. The molecules studied here are especially interesting because their excited electronic states are Rydberg in nature and the structural differences among them are relatively minor.

The binding mechanism of an excimer or exciplex (*excited complex*) is of theoretical interest. Two models have been proposed to account for the attractive forces in excimers and exciplexes. One is charge resonance, which is essentially coulombic in nature. The other, exciton resonance, derives its attractiveness through an interaction of transition dipoles. It has been stated that neither of the two mechanisms can, alone, account for the bound states observed in the aromatic excimers.[4]

Recent discussions of the concept of 3-electron bonds[5] are, perhaps, conducive to a better understanding of the excimer state. In the saturated amine excimers, which are derived from excited monomers whose upper states are Rydberg in nature, one encounters a σ-bonded system involving a quasi-ionized and neutral amine pair. Thus, in the limit, the amine excimers are akin to association complexes between radical cation and neutral species, e.g., as observed in certain sulfides,[6a,b] phosphines,[6c-g] and arsines.[6c,h] The amine excimers are more closely related to the saturated amine dimer radicals proposed in flash photolysis studies[7] and observed recently by Dinnocenzo in low-temperature EPR studies.[8] Moreover, considerable information and understanding has been provided by Alder et al. about this type of interaction between N atoms in structurally constrained diamine cations.[9a-k] Thus, association in the saturated amine excimers may be regarded as an example of 3-electron bonding in a *neutral* molecular system. The 3-electron σ-bond nature of these excimers is more explicitly embraced in the model to be described below. It is hoped that this work will further the understanding of the binding mechanism in saturated amine excimers.

In the past, considerable experimental work has been aimed at characterizing these excimers; however, relatively little effort has been applied to developing theoretical models for interpreting these observations. In the present study, MNDO and AM1 calculations are used to help rationalize the differences in the measured binding energies of the cage amine excimers. Attention is focused on the relationship between the structure of an amine and its excimer binding energy. We also present, for the first time, evidence for the existence of the **322** excimer in *n*-hexane solution. An interpretation of the trend in excimer binding properties of these compounds is presented. **DA222**, which fails to manifest excimer formation, is contrasted with **222**, and an explanation for this difference is discussed.

Experimental Section

322 was furnished through the cooperation of Professor Lee Flippen. The synthetic route employed is as follows:

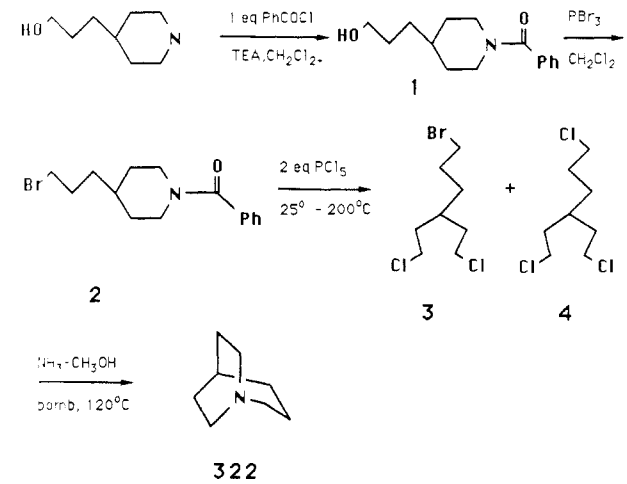

***N*-Benzoyl-4-(3-hydroxypropyl)piperidine (1).** To a stirred, 273 K solution of 4-(3-hydroxypropyl)piperidine (79.00 g; 0.552 mol) and dry triethylamine (154 mL; 1.14 mol) in 400 mL of methylene chloride was added 64.0 mL (0.552 mol) of benzoyl chloride over 20 min. After 1 h a simple extractive workup gave 131.06 g (96%) of **1**, which required no further purification for use in the preparation of **2**.

***N*-Benzoyl-4-(3-bromopropyl)piperidine (2).** Phosphorus tribromide (19.0 mL; 0.20 mol) was added dropwise over 15 min to a stirred solution of **1** (41.46 g; 0.168 mol) in 50 mL of methylene chloride at 293 K. The reaction mixture was allowed to warm to room temperature, and after 16 h the reaction was quenched slowly with ice-cold saturated $NaHCO_3$. (*Caution*! Exothermic reaction!) An extractive workup of the crude product afforded 41.05 g of **2** as a yellow oil. This material crystallized on standing and was pure (39.73 g; 76%) after titration with pentane.

1-Azabicyclo[3.2.2]nonane (322). Treatment of **2** under von Braun reaction conditions[10] afforded, in the best instance, a 2:1 mixture of 6-bromo-3-(2-chloroethyl)-1-chlorohexane (**3**) and 3-(2-chloroethyl)-1,6-dichlorohexane (**4**), respectively, in 51% total yield. This mixture of trihalides was used to alkylate ammonia essentially by the method of Prelog.[11] Thus, reaction of 7.42 g of the 2:1 mixture of **3** and **4** with 30 mL of liquid NH_3 in 50 mL of methanol (sealed bomb, 393 K, 2.5 h) afforded a crude, brown semisolid product. This material was dissolved in 15 mL of 40% methanolic KOH, and the resulting solution was concentrated with a rotary evaporator. The residue was extracted with five portions of ether; the combined ether layers were dried ($MgSO_4$), filtered, and concentrated with a rotary evaporator. The brown, oily residue thus obtained was bulb-to-bulb distilled under reduced pressure to afford 1.69 g (45%) of **322**. This material was further purified by preparative GLC to afford analytically pure samples of **322**.

For the photophysical studies, the amine was first dissolved in 2-methylbutane and dried with lithium aluminum hydride (LAH). The 2-methylbutane was evaporated and the base twice sublimed under high vacuum. **322** was removed from the cold finger in a dry N_2 atmosphere. The same sample preparation procedure was followed for all experiments. *n*-Hexane (Burdick and Jackson UV grade) was dried over LAH and passed through approximately 25 cm of argentated alumina before use. There was negligible solvent absorbance in the spectral region examined (down to ca. 215 nm). Fluorescence samples were deaerated with dry N_2 gas for 2 min. Concentrations were determined spectrophotometrically on deaerated samples. For the photophysical experiments involving **DA222**, a 2×10^{-2} M 2-methylbutane solution was prepared containing a small amount of LAH to avoid any complications caused by the **DA222**/H_2O exciplex.[12]

(4) Birks, J. B. *Photophysics of Aromatic Molecules*; Wiley-Interscience: London, 1970; p 38.

(5) (a) Hub, W.; Schneider, S.; Dorr, F.; Oxman, J.; Lewis, F. D. *J. Am. Chem. Soc.* **1984**, *106*, 708. (b) Harcourt, R. D. *Aust. J. Chem.* **1978**, *31*, 199.

(6) (a) Asmus, K. *Acc. Chem. Res.* **1979**, *12*, 437. (b) Gerson, F.; Knöbel, J.; Buser, U.; Vogel, E.; Zehnder, M. *J. Am. Chem. Soc.* **1986**, *108*, 3781. (c) Symons, M. C. R. *Mol. Phys.* **1972**, *24*, 885. (d) Lyons, A. R.; Symons, M. C. R. *J. Chem. Soc., Faraday Trans. 2*, **1972**, *68*, 1589. (e) Gillbro, T.; Kerr, C. M. L.; Williams, F. *Mol. Phys.* **1974**, *28*, 1225. (f) Claxton, T. A.; Fullman, B. W.; Platt, E.; Symons, M. C. R. *J. Chem. Soc., Dalton Trans.* **1975**, 1395. (g) Symons, M. C. R.; McConnachie, G. D. G. *J. Chem. Soc., Chem. Commun.* **1982**, 851. (h) Hudson, R. L.; Williams, F. *J. Phys. Chem.* **1980**, *84*, 3483.

(7) Halpern, A. M.; Forsyth, D. A.; Nosowitz, M. *J. Phys. Chem.* **1986**, *90*, 2677.

(8) Dinnocenzo, J. P.; Banach, T. E. *J. Am. Chem. Soc.* **1988**, *110*, 971.

(9) (a) Alder, R. W.; Sessions, R. B. *The Chemistry of Amino, Nitroso, and Nitro Compounds*; Patai, S., Ed.; Wiley: New York, 1982; Part 2, pp 762–804. (b) Alder, R. W. *Acc. Chem. Res.* **1983**, *16*, 321. (c) Alder, R. W.; Goode, N. C.; King, T. J.; Mellor, J. M.; Miller, D. W. *J. Chem. Soc., Chem. Commun.* **1976**, 173. (d) Alder, R. W.; Gill, R.; Goode, N. C. *J. Chem. Soc., Chem. Commun.* **1976**, 973. (f) Alder, R. W.; Sessions, R. B.; Mellor, J. M.; Rawlins, M. F. *J. Chem. Soc., Chem. Commun.* **1977**, 747. (g) Alder, R. W.; Sessions, R. B. *J. Am. Chem. Soc.* **1979**, *101*, 3651. (h) Alder, R. W.; Casson, A.; Sessions, R. B.; Asmus, K.-D.; Hiller, K.-O.; Gobl, M. *J. Am. Chem. Soc.* **1980**, *102*, 1429. (i) Alder, R. W.; Arrowsmith, R. J.; Casson, A.; Sessions, R. B.; Heilbronner, E.; Koval, B.; Huber, H.; Taagepera, M. *J. Am. Chem. Soc.* **1981**, *103*, 6137. (j) Alder, R. W.; Orpen, A. G.; Sessions, R. B. *J. Chem. Soc., Chem. Commun.* **1983**, 999. (k) Alder, R. W.; Sessions, R. B.; Gmunder, J. O.; Grob, C. A. *J. Chem. Soc., Perkin Trans 2* **1984**, 411.

(10) (a) Hageman, H. A. *Org. React. (N.Y.)* **1953**, *7*, 198. (b) von Braun, J. *Org. Syntheses*; Wiley: New York, 1941; Collect. Vol. I, p 428.

(11) Cerkovnikov, E.; Prelog, V. *Liebigs Ann. Chem.* **1937**, *83*, 532.

(12) Halpern, A. H.; Ruggles, C. J.; Zhang, X. *J. Phys. Chem.* **1987**, *109*, 3748.

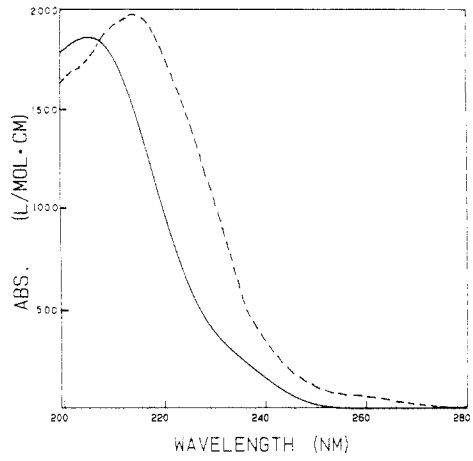

Figure 1. Absorption spectra of **222** (—) and **322** (---).

The quantum efficiency of the monomer was obtained at low concentration (ca. 10^{-5} M) and 296 K. A quantum efficiency of 0.47 was calculated for the **322** monomer by comparing the integrated fluorescence spectrum of **322** with that of of 1.5×10^{-4} M *n*-hexane solution of triethylamine (TEA). We assume a quantum efficiency of 0.69 for TEA. The value of the intrinsic excimer fluorescence quantum efficiency, q_{fD}, of 0.02 was obtained at 296 K by using the excimer emission of a concentrated **222** solution as a standard. The relationship used to determine q_{fD} is

$$q_{fD} = \Phi_{fD}\left[1 + \frac{k_M(k_D + k_{MD})}{k_D k_{DM}[M]}\right]$$

where Φ_{fD} is the measured quantum yield of the **322** excimer relative to the **222** standard. The rate constants are described below.

Due to differences in the absorption spectra (vide infra), a 1.2 M solution of **222** was required to match the absorbance of the **322** at an appropriate wavelength (260.0 nm) where the absorbance is less than 0.2. The **222** solution was calibrated with a 1,1′-binaphthyl solution to obtain an absolute value of the fluorescence yield for the **222** excimer. In all cases the fluorescence intensities were corrected for light absorption. 1,1′-Binaphthyl (Eastman Kodak Co.) was sublimed prior to use.

The MNDO and AM1 approximations, described by Dewar et al.,[13] are used in calculations performed for both the amine monomers and the excimer models of **221**, **222**, and **322**. Most of the work was carried out on a VAX 11/780 computer. Full-optimizations of the coordinates of both the **222** and **DA222** cation/neutral dimers were performed on a VAX 8800. The jobs were run over the period of several days with numerous restarts due to the large amount of CPU time required, e.g., up to 40 h for a full **222** radical–neutral dimer optimization.

Decay curves were obtained by the time-correlated single-photon counting method.[14] The instrument has been previously described.[15] Briefly, however, the sample was excited with the dispersed (3.2-nm band-pass) emission of a gated D_2 flashlamp (0.5 atm) at 30 kHz. Fluorescence was isolated with interference filters (Corion Corp.) having transmission maxima at 285 (monomer) and 360 nm (excimer). The cell temperature was regulated with a thermoelectric device driven by a homemade proportioning controller. Temperature stability and accuracy was ±0.1 K. To obtain the low-temperature data of **DA222**, a fluorescence cell containing **DA222** solution was placed in a Suprasil Dewar flask into which cold N_2 vapor boiled off of liquid N_2 was passed. Temperature accuracy and stability of this apparatus was ±2.0 K. When decay curves were acquired, the optimal excitation wavelength was determined empirically by adjusting the excitation monochromator until a maximum count rate was achieved. The decay parameters for a given sample pumped at different wavelengths did not vary significantly. The decay curves were analyzed on a LSI 11/23 computer system using the reconvolution method of Frye et al.[15]

Uncorrected fluorescence spectra were obtained with a dc fluorometer equipped with a D_2 source (excitation and emission band-pass, 3.2 and 2.0 nm, respectively) described previously.[2] Absorption spectra were acquired on a Varian 2300 scanning spectrophotometer.

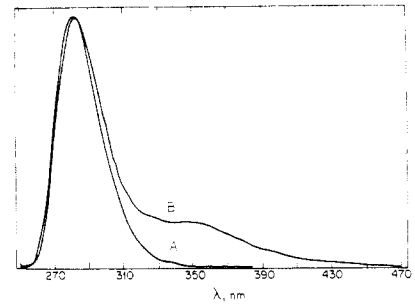

Figure 2. Emission spectra of **322** showing both monomer emission (A; 1.0×10^{-5} M) and excimer emission (B; 1.0×10^{-2} M).

Results and Discussion

The absorption spectrum of **322** in *n*-hexane solution is generally similar to the solution-phase spectra of other tertiary monoamines. This similarity can be seen in Figure 1, which contains the absorption spectra of **322** and **222**. The spectra displayed contain both $S_1 \leftarrow S_0$ and portions of the much stronger $S_2 \leftarrow S_0$ transitions for each compound. $S_1 \leftarrow S_0$ maxima are not observed for either compound; however, the Frank–Condon maximum for the $S_2 \leftarrow S_0$ transition of **322**, being red shifted, is observed at 215 nm. The $S_2 \leftarrow S_0$ maximum is at 205 nm in the **222** spectrum; the steep absorption that starts to overlap a weaker transition at ca. 230 nm is assigned as the leading edge of the $S_2 \leftarrow S_0$ transition.

The first two electronic transitions of these compounds have been described as Rydberg in nature, originating on the N atom and consisting of (n, 3s) and (n, 3p) promotions, respectively.[16] The red shift in the absorption spectrum of **322** can be viewed as a consequence of the destabilization of the n orbital caused by an increase in the C–N–C angle as one of the bridges extended. Consistent with this interpretation is the fact that the origins of the $S_1 \leftarrow S_0$ and $S_2 \leftarrow S_0$ transitions of gas-phase **322** are at 264.6 and 239.9 nm, i.e., 1401 and 2174 cm^{-1} lower in energy than the respective transitions of **222**. A further result of n-orbital destabilization in **322** is that, assuming constant term values, the ionization potential of **322** is expected to be 7.40 eV, 0.32 eV lower than that of **222** (7.72 eV, adiabatic).[17]

As with the difference in the absorption spectra, there is also a shift to lower energies in the fluorescence spectrum of **322** vis-à-vis **222** at low concentration (ca. 1×10^{-5} M), in *n*-hexane solution. The fluorescence maximum of **322** appears at 282 nm, as compared with 272 nm for **222**. This difference is consistent with the above observation that the S_1–S_0 gap is smaller in **322** than in **222**.

Significantly, however, at higher concentrations (ca. 1×10^{-2} M), the fluorescence spectrum of **322** is distinctly different relative to the dilute solution spectrum. At high concentration, additional emission is observed at longer wavelengths (ca. 350 nm) than the fluorescence maximum. This long-wavelength emission is displayed in spectrum B in Figure 2. This emission was not previously detected presumably because of the high concentration necessary for its observation.[2] The possibility that this red-shifted emission is due to a ground-state dimer is precluded by the concentration independence of the absorption spectrum. For this, and other, more direct reasons (vide infra), the long wavelength emission is assigned as **322** excimer fluorescence.

Monomer/excimer systems, in addition to exhibiting concentration-dependent emission spectra (often a distinct, red-shifted maximum), also show, under appropriate conditions, double-exponential fluorescence decay. Fluorescence decay curves of a 1.1×10^{-3} M **322** solution at 263 K, analyzed at 285 and 360 nm (where monomer emission is negligible, see Figure 2), are shown

(13) (a) Dewar, M. J. S.; Thiel, W. *J. Am. Chem. Soc.* **1977**, *99*, 4899. (b) Dewar, M. J. S.; Zoebisch, E. G.; Healy, E. F.; Stewart, J. J. P. *J. Am. Chem. Soc.* **1985**, *107*, 3902.

(14) O'Conner, D. V.; Phillips, D. *Time-Coorelated Single Photon Counting*; Academic: London, 1984.

(15) Frye, S. L.; Ko, J.; Halpern, A. H. *Photochem. Photobiol.* **1984**, *40*, 555.

(16) Robin, M. B. *Higher Excited States of Polyatomic Molecules*; Academic: New York, 1974; Vol. 1, pp 208–229.

(17) Halpern, A. M.; Roebber, J. L.; Weiss, K. *J. Chem. Phys.* **1968**, *49*, 1348.

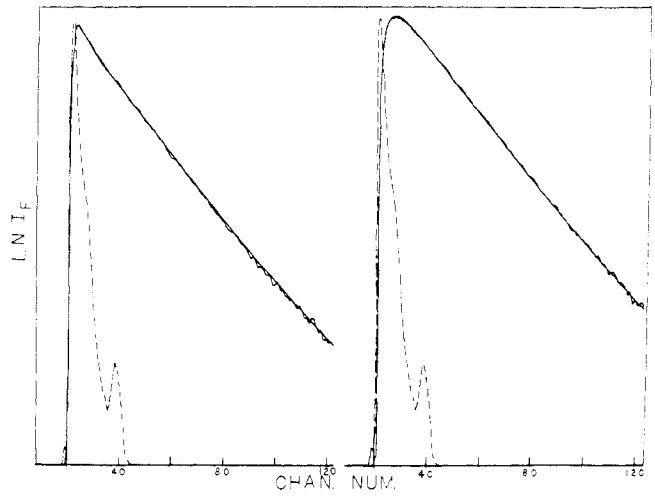

Figure 3. Fluorescence decay curves of **322** monomer and excimer obtained at 263 K (1.1×10^{-3} M) and fit over three decades of intensity: lamp curve (---). χ^2 for the combined fit is 3.30.

Scheme I

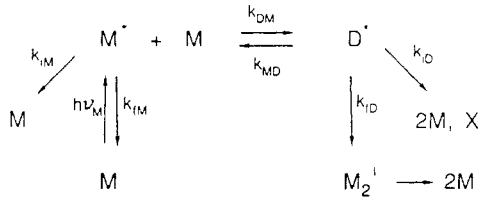

in Figure 3. Reconvolution analyses indicate that the short- and long-wavelength emissions (monomer and excimer, respectively) can be represented by the decay laws $I_M(t) = \exp(-23.4/t) + 0.581 \exp(-43.0/t)$ and $I_D(t) = \exp(-23.4/t) - 1.01 \exp(-43.0/t)$ where t is in nanoseconds.

The kinetic scheme used to represent the photophysical behavior of **322** is shown in Scheme I. The notation is that of Birks[4] where k_{fM} and k_{fD} are the radiative rate constants for M* and D*, respectively, and k_{iM} and k_{iD} are the corresponding nonradiative rate constants. The bimolecular excimer formation rate constant is denoted as k_{DM}; k_{MD} is the unimolecular rate constant for the dissociation of the excimer.

From the decay curves shown in Figure 3, one can see the distinctly different time dependencies of the long- and short-wavelength regions of **322** fluorescence spectrum. The results given above are consistent with the predictions of the solutions of the coupled differential equations for the kinetic scheme[4] that (a) the values of λ_1 and λ_2 be common to both monomer and excimer and (b) the long-wavelength decay curve have a −1 ratio of the two exponential components. These facts, along with the concentration dependence of the emission spectrum, confirm the assignment of the long-wavelength emission as originating from the **322** excimer.

Determination of Rate Constants. The rate constants of the **322** monomer/excimer system were determined from a combination of both transient and steady-state experiments. In the transient experiments, the rate constants were determined by examining the concentration and temperature dependence of the decay parameters λ_1, λ_2, and A. Due to the considerably restricted concentration and temperature regimes where double-exponential decay curves could be accurately measured, not all rate constants could be satisfactorily extracted from transient experiments. To complement the determination of the rate constants, steady-state experiments were also performed. When the temperature dependence of the total fluorescence spectrum (see Figure 2) is examined, an expression involving the rate constants can be determined and used to test the consistency of the results of transient experiments.

The monomer decay rate constant, k_M, was directly obtained from the low-concentration ($<10^{-5}$ M) fluorescence decay analyzed

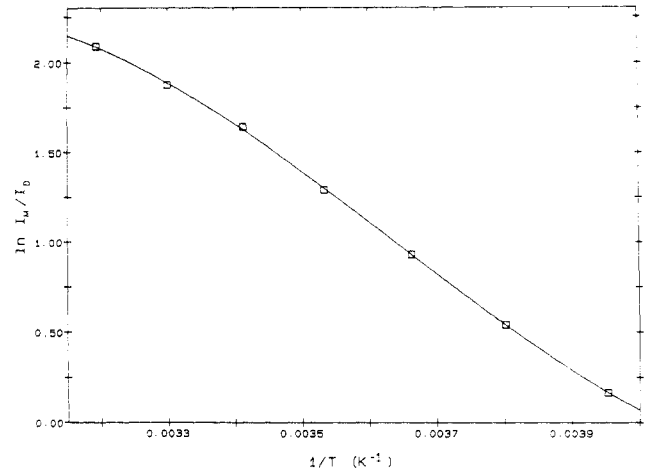

Figure 4. Temperature dependence of the ratio of monomer to excimer emission intensities.

Table I. *A* Factors and Temperature Dependences of the Photophysical Rate Constants for the **322** Monomer and Excimer

monomer		excimer		formation–dissociation	
A_{fM}	7.5×10^6	A_{fD}	1.5×10^6	A_{DM}[b]	6.6×10^{11}
W_{fM}[a]	0	W_{fD}	0	W_{DM}	7.9
A_{iM}	8.5×10^6	A_{iD}	8.7×10^{10}	A_{MD}	1.0×10^{15}
W_{iM}	0	W_{iD}	18.4	W_{MD}	30.1

[a] W is given in kJ/mol. [b] A_{DM} is given in M^{-1} s^{-1}. All others are in s^{-1}.

at 285 nm. Under these conditions, monomer decay is single exponential and may be considered to be unquenched. Consequently, $k_M \simeq \lambda_2$, i.e., 1.6×10^7 s^{-1}. k_M, determined in this manner, was found to be invariant over the temperature range 263–313 K. When $q_{fM} = 0.47$ is used in the equation $k_{fM} = q_{fM}k_M$, k_{fM} and k_{iM} are found to be 7.5×10^6 and 8.5×10^6 s^{-1}, respectively.

From an analysis of the decay parameters,[3] k_D was found to increase with temperature. Accordingly, the standard expression concerning the temperature dependence of the monomer and excimer emission spectra[18] must be modified. When the Arrhenius forms for the rate constants where A is a preexponential term and W is the activation parameter are used and k_{fM} is assumed to be temperature independent, the temperature dependence of the emission spectrum is as indicated in eq 1. In Figure 4, eq 1 has

$$I_M/I_D = \frac{A_{fM}[A_D \exp(-W_D/RT) + A_{MD} \exp(-W_D/RT)]}{[A_{fD} \exp(-W_{fD}/RT)][A_{DM} \exp(-W_{DM}/RT)][M]} \quad (1)$$

been fit to the I_M/I_D data. The values of the rate constants obtained from the steady-state experiments are satisfactorily consistent with those obtained from the transient experiments. These rate constants are summarized in Table I.

Discussion of Rate Constants. As reported above, k_M is temperature independent; this property is consistent with previous observations of other amines.[3] k_{DM} has an activation energy of 7.9 kJ/mol, which is consistent with a diffusion-controlled process in *n*-hexane solution. Interestingly, excimer decay appears to be relatively strongly activated with $W_D = 18.4$ kJ/mol. To determine the origin of this activation, the excimer fluorescence intensity, I_D, was examined. When Arrhenius forms for the rate constants are used, the expression for I_D is as indicated in eq 2. Thus, I_D

$$I_D = \frac{q_{fD}}{1 + \dfrac{k_M(k_D + k_{MD})}{(k_{fD} + k_{iD})k_{DM}[M]}} \quad (2)$$

(18) Stevens, B.; Ban, I. M. *Trans. Faraday Soc.* **1964**, *60*, 1515.

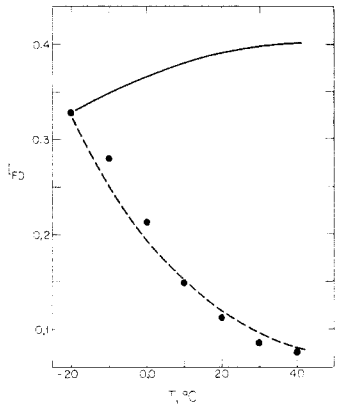

Figure 5. Temperature dependence of excimer fluorescence intensities with the temperature dependence explicitly placed in k_{fD} (—) or k_{iD} (---) observed data (●).

can be plotted as a function of temperature to determine whether the activation of k_D stems from k_{iD} or k_{fD}. In Figure 5, such a plot is displayed with the temperature dependence of k_D placed either in k_{iD} or k_{fD}. It is clear from the comparison in Figure 5 that the temperature dependence of the excimer decay can be assigned to a nonradiative process. It should be noted that similar behavior has been observed for the **222** excimer.[3]

The temperature dependence of k_{MD} is governed by the binding energy of the excimer, B, which is defined as $W_{MD} - W_{DM}$, the difference in the activation energies of the dissociation and formation rate constants. We have determined a binding energy of 22.2 kJ/mol for the **322** excimer, and this compares with 36.8 kJ/mol for the **222** excimer.[3] As a result of a large binding energy, an *n*-hexane solution of **221** at room temperature fluoresces with a single-exponential decay. Due to the single-exponential behavior, transient studies are of little assistance in characterizing the excimer. However, at elevated temperatures (400–500 K) where k_{MD} is comparable to k_D, the binding energy of **221** in hexadecane solution has been reported to be 51.0 kJ/mol on the basis of a steady-state approach.[2]

In an attempt to determine the extent to which excimer formation is common among the cage amines, **333** was also examined. Extensive analysis of the fluorescence spectra and decay curves of the **333** homologue fails to reveal evidence of excimer emission. The **333** samples were rigorously dried to prevent the formation of the emissive **333***···H_2O exciplex, which leads to nonexponential decay and spectral broadening. These studies were made under conditions of high concentration and low temperature (e.g., 1.5×10^{-2} M in *n*-hexane at 263 K) where the excited-state equilibrium would be shifted to favor the excimer. The lack of an emissive excimer not withstanding, **333** is observed to undergo self-quenching at the diffusion-controlled rate in *n*-hexane at room temperature.

We now consider the trend in the binding characteristics of the bicyclic amine excimers. As a given bridge is extended by additional methylene units, there is a decrease in the excimer binding energy. We suggest that this decrease is due to increased steric interaction between the α-carbon hydrogen atoms of the monomer subunits. Observations about the role of steric hindrance in excimer formation have been reported for methyl-substituted benzenes.[19] To understand how the amine excimer binding energy is affected by additional methylene units, differences in molecular geometry must be considered. As the bridge is extended, two changes in geometry can be noted: (1) there is an increase in the C–N–C bond angles, and (2) there is a decrease in the dihedral angle formed by the lone pair of electrons and the nitrogen, carbon, and hydrogen atoms. Both of these structural changes increase the degree to which the α-carbon hydrogen atoms interact, resulting in larger repulsive forces upon excimer formation. In an attempt to model the effect of these geometrical changes on excimer formation, computational methods were employed.

Calculations. Part of our objective is to use a theoretical model that can explain trends in excimer binding energies discussed above. As mentioned above, the Rydberg nature of the electronically excited states of saturated amines suggests that the radical cation can be used to represent the excited species.

Accordingly, a cation–neutral ($M^{\bullet+}\cdots M$) or ($M\cdots M)^{\bullet+}$ model was chosen to evaluate structural effects on amine excimer stability. Another reason for using the cation to represent the electronically excited state in the amines is that the extravalence orbitals presumably needed to describe the Rydberg states (e.g., (n_N, 3s) are not accounted for in the MNDO and AM1 methods. The geometries of both the cation and neutral were first optimized individually by an unrestricted Hartree–Fock Hamiltonian in the MNDO approximation. Subsequently, the cation- and neutral-optimized coordinates were combined for use in a "dimer" calculation. The axis of approach was chosen to contain both nitrogen atoms and to be normal to the planes defined by the α-carbon atoms of each molecule with the nitrogen atoms facing one another. In the cases where the molecules lack rotational symmetry (i.e., **221** and **322**), the odd-membered bridges were fixed in an anti orientation, which presumably minimizes steric repulsion. The same reasoning being used, the α-carbon atoms of **222** were oriented in a staggered position. Additional calculations were done to verify that these "head-to-head" orientations represent absolute minima (vide infra).

In most calculations, neutral and cation geometries were held fixed because the number of atoms in the dimers (e.g., 48 for **322**) made full optimization impractical for all systems studied. The implicit assumptions in adopting these geometries are (1) the cation has a geometry similar to that of the S_1 electronic state and (2) the geometries of each of the two species M and M* do not change upon the formation of the excimer D*. The first assumption can be supported on the basis that S_1 has been assigned as a 3s Rydberg state. In the calculations of the **222** neutral–cation pair, in which coordinates were globally optimized, both AM1 and MNDO indicate that the charged and neutral molecular components retain geometries and atomic charges close to those of the respective separated species. Results of an EPR study of the **222** dimer cation, however, indicate that the two N atoms are equivalent on the EPR time scale.

The results of the separate neutral and cation geometry optimizations for these three amines show significantly different structures not only among the three compounds but also between the cation and neutral of a given molecule. With respect to the three neutral amines, the calculations predict increasing C–N–C bond angles for **221**, **222**, and **322**. MNDO calculations also predict a change in the C–N–C bond angles upon ionization for these three amines. An increase in C–N–C bond angle upon ionization is consistent with the planar equilibrium geometries of saturated acyclic amines in their electronically excited states. Values for the optimized C–N–C angles for the three bicyclic amines, and relevant experimental data are summarized in Table II.

To further examine the effect of the geometrical changes mentioned above on excimer stabilization, optimized neutral and cation coordinates were combined to afford cation–neutral pair coordinates with differing N–N separations. The results of such an analysis predict a bound state for each of the three monoamine cation–neutral pairs. For each cation–neutral pair, energies were calculated for N–N separations. The calculated energies of the dimers, separated by 10 Å, are in agreement (<0.1%) with the sum of the energies of the individual optimized cation and neutral species. The results of these comparisons for the three amines studied are parallel to the observation that as a bridge is extended, the binding energies of these excimers decrease. By fitting these

(19) Birks, J. B.; Braga, C. L.; Lumb, M. D. *Proc. R. Soc. London, A* **1965**, *283*, 84.
(20) Chiang, J. F.; Wilcox, C. F., Jr; Bauer, S. H. *J. Am. Chem. Soc.* **1968**, *90*, 3144.
(21) Johnson, L. *J. Chem. Phys.* **1960**, *33*, 949.
(22) Bruesch, P. *Spectrochim. Acta* **1966**, *22*, 867.
(23) Amizel, L. M.; Baggio, S.; Baggio, R. F.; Becka, L. N. *Acta Crystallogr., Sect. B: Struct. Crystallogr. Cryst. Chem.* **1974**, *30*, 2494.

Table II. C–N–C Bond Angles for **221**, **222**, and **322**

	neutral			cation		
	C_6–N–C5	C6–N–C1	C1–N–C5	C6–N–C5	C6–N–C1	C1–N–C5
			221			
exptl[a]	101	101	103			
MNDO	101.6	101.7	109.3	107.8	107.7	117.0
			222			
exptl[b]	109	109	109			
MNDO	110.1	110.1	110.0	115.2	115.6	115.1
			322			
exptl[c]	115	115	110			
MNDO	115.1	115.0	112.1	119.3	119.3	115.8

[a] From norbornane.[20] [b] See ref 21 and 22. [c] From 3-azabicyclo[3.2.2]nonane.[23]

nine energies to a Morse potential, one obtains well depths (binding energies) of 17.5, 16.1, and 10.8 kJ/mol for **221**, **222**, and **322**, respectively. Binding energies obtained from MNDO calculations follow the trend in the experimentally observed values. While the trend is correctly predicted, the calculations indicate considerably lower binding strengths than those observed. This may be attributed to the fact that MNDO has a tendency to overestimate steric interactions[24] or that higher states are not included in the calculation precluding any stabilization arising from an exchange interaction of the singly populated nitrogen 3s orbitals. We performed calculations on the **222** dimer cation using the AM1 Hamiltonian for comparison with the MNDO results. The AM1 calculation on the globally minimized system indicates that the dimer cation is more stable by 13.4 kJ/mol relative to the MNDO method; the arrangement of the two amines, however, is not collinear in this case. When constrained to a (staggered) collinear geometry, the dimer cation is still more stable with AM1 (by 10.1 kJ/mol).

The hypothesis that the α-carbon hydrogen atoms play a major role in affecting the binding strength of the cage amine excimers is further supported by calculations involving the ground-state interaction of a pair of amines. MNDO calculations were performed on two *neutral* amines, one with a cation geometry and the other having a neutral geometry. The results, as expected, show that the total energy increases as the molecules are brought closer together. What should be noted is that, as methylene units are added to a bridge of a cage amine, the repulsions are greater for a given N–N separation. Although calculations have not been performed for **333**, molecular models suggest that the trend observed in the smaller cage amines continues. The geometries used for the neutral–neutral calculation are depicted in Figure 6, where the N–N separation is chosen to be 1 Å for the purpose of illustration. One can see from Figure 6 that the degree of interaction between the α-carbon hydrogens increases as the number of methylene units in a bridge increase.

We now consider the properties of **DA222**. In contrast with **222**, which forms a strongly bound, fluorescent excimer (36.8 kJ/mol), we have found that the diamine does not reveal evidence of photoassociation. The fluorescence lifetime of **DA222**, in *n*-hexane solution at 300 K is concentration independent; 81 ns between 10^{-5} and about 0.1 M (saturation). Moreover, the fluorescence lifetime of **DA222** in high concentration (2.0×10^{-2} M) 2-methylbutane solution is nearly temperature independent between 230 and 300 K and can be accounted for by changes in solvent density (i.e., refractive index). In addition, the position and shape of the fluorescence spectra were observed to be invariant.

The failure **DA222** to manifest excimer formation and even undergo appreciable self-quenching ($k_q < 10^7$ M^{-1} s^{-1}) appears surprising. The steric arguments cited above cannot account for these observations because of the similar C–N–C bond angles and α-carbon hydrogen atom orientations vis-à-vis **222**. We interpret the inability to observe the excimer of **DA222** as arising from the inherently higher stability of the (lowest) excited state of this diamine with respect to association with its ground-state counterpart. Our model calculations, performed on the **DA222** dimer radical, imply that the excimer stabilization of this system would be less than half that of **222**. Because of the relatively low solubility of **DA222** in alkane solvents, we presumably cannot prepare a system (i.e., concentration/temperature) in which excimer concentration is large enough to allow its observation.

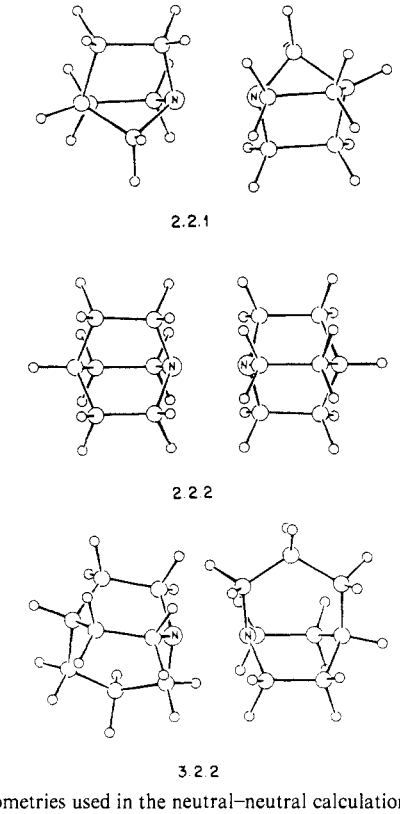

Figure 6. Geometries used in the neutral–neutral calculations illustrating the orientations of the interacting α-carbon hydrogens. The N–N separation was chosen as 1 Å in each case. In these representations the neutral constrained to a cation geometry is depicted on the right-hand side.

The inertness of **DA222** with respect to self-quenching and excimer formation, and the smaller binding energy of its dimer radical vis-à-vis **222**, can be rationalized in terms of the lower gas-phase basicity of the diamine. Staley and Beauchamp,[25] using the criterion of the homolytic bond dissociation energy [$D(B^+–H)$] of the protonated gas-phase amine as a measurement of its basicity, determined that **DA222** is a weaker base than **222** by ca. 60 kJ/mol. They interpreted this result in terms of the resonance stabilization of the **DA222** radical cation, a property arising from the coupling between the two n_N orbitals. This result was qualitatively confirmed by Alder et al.[9i] Alternatively viewed, in the **DA222** radical cation, the "hole" density on each N atom is smaller than that in **222** because of the strength of the N–N

(24) Clark, T. *A Handbook of Computational Chemistry*; Wiley: New York, 1985.

(25) Staley, R. H.; Beauchamp, J. L. *J. Am. Chem. Soc.* **1974**, *96*, 1604.

coupling in the diamine. If one considers the hole of the cation as delocalized on the two nitrogen atoms, then via a coulombic argument the **DA222** cation–neutral pair would have a much lower stabilization than the analogous **222** pair. This idea can be applied mutatis mutandis to the excited electronic states of these compounds.

Finally, it is interesting to compare the photophysics of the cage amines with those of the acyclic tertiary amines. Excimer formation has been observed in only one acyclic amine: the diamine *N,N,N',N'*-tetramethyl-1,3-propanediamine (TMPD) whose binding energy has been reported to be 11.3 kJ/mol.[26] While no direct evidence of excimer formation has been observed for any other acyclic amines, there is, nevertheless, some interesting behavior. For example, triethylamine (TEA) in *n*-hexane solution has a fluoroescence self-quenching rate constant of 6×10^9 M^{-1} s^{-1}, about one-third the diffusion-controlled value. Due to the similarity in amine geometries, one would expect TEA to have an association with a stability approximately equal to that of TMPD. The fact that excimer fluorescence is not observed in TEA is probably due to steric interactions between the alkyl groups of the planer, excited-state molecule and those of the ground-state monomer. Rapid conformational interconversion of the ground state as discussed by Bushweller et al.[27] would also presumably inhibit excimer formation. As the self-quenching rate constant suggests, a weakly bound excimer may play a role in the fluoresence quenching process.

It is evident from photophysical studies that amine excimer stabilization is decreased as methylene units are added to the bridge of the cage. This observation is explained as arising from an increase in steric hindrance to excimer formation. This hindrance has been determined to be brought about by increases in both the C–N–C angles and the lone-pair N–C–H dihedral angle as methylene units are added. Regarding **DA222**, an argument based on electronic structure can be made to account for the lack of excimer formation. While emissive excimers are found in relatively few amines, it is possible that weak photoassociation occurs in many of the tertiary amines.

Acknowledgment. The donors of the Petroleum Research Fund, administered by the American Chemical Society, provided partial support for this work. We express our gratitude to Dr. A. Ames of the Polaroid Corp. for his generosity and help in performing calculations on the VAX 8800. We also acknowledge Dr. D. Forsyth for helpful discussions and Dr. L. Flippen for providing us with **322**.

(26) Halpern, A. M.; Chan, P. P. *J. Am. Chem. Soc.* **1975**, *97*, 2971.

(27) Bushweller, C. H.; Fleischman, S. H.; Grady, G. L.; McGoff, P.; Rithner, C. D.; Whalon, M. R.; Brennan, J. G.; Marcantonio, R. P.; Domingue, R. P. *J. Am. Chem. Soc.* **1982**, *104*, 6224.

The Rapid Hydration of the Acetyl Radical. A Pulse Radiolysis Study of Acetaldehyde in Aqueous Solution

Man Nien Schuchmann and Clemens von Sonntag*

Contribution from the Max-Planck-Institut für Strahlenchemie, Stiftstr. 34-36, D-4330 Mülheim a.d. Ruhr, Federal Republic of Germany. *Received February 10, 1988*

Abstract: In aqueous solution acetaldehyde and its hydrate are in a 0.8:1 equilibrium. Hydroxyl radicals generated by the pulse radiolysis of N_2O-saturated water react with this mixture with an overall rate constant of $k = 2.4 \times 10^9$ dm^3 mol^{-1} s^{-1}, the rate of reaction with acetaldehyde being about 3 times faster ($k_5 = 3.6 \times 10^9$ dm^3 mol^{-1} s^{-1}) than with the hydrate ($k_6 = 1.2 \times 10^9$ dm^3 mol^{-1} s^{-1}). The predominant radicals formed are the acetyl radical and its hydrated form, H-abstraction at methyl occurring to only about 5–10%. The acetyl radical rapidly hydrates ($k_9 = 2 \times 10^4$ s^{-1}). Thus, its rate of hydration is 2×10^6 times faster than that of the parent compound acetaldehyde. The hydrated acetyl radical has been monitored by its rapid reduction of tetranitromethane ($k_{11} = 2.8 \times 10^9$ dm^3 mol^{-1} s^{-1}), the formation of $O_2^{\bullet-}$ in the presence of oxygen, and its deprotonation at pH 11 ($pK_a \leq 9.5$). The acetyl radical does not oxidize *N,N,N',N'*-tetramethyl-*p*-phenylenediamine (TMPD) at the pulse radiolysis time scale, but the acetylperoxyl radical (formed in the presence of oxygen) reacts rapidly with TMPD ($k_{15} = 1.9 \times 10^9$ dm^3 mol^{-1} s^{-1}), ascorbate ($k = 8.3 \times 10^8$ dm^3 mol^{-1} s^{-1}), and $O_2^{\bullet-}$ ($k_{16} \simeq 10^9$ dm^3 mol^{-1} s^{-1}) and hence is the most strongly oxidizing peroxyl radical known so far. Data on the rate of water loss from the hydrated acetyl radical are considerably less accurate, but it may well be that this reaction has a rate constant of $k_{10} \simeq 3 \times 10^4$ s^{-1}.

In aqueous solutions acetaldehyde is present in a 0.8:1.0 mixture of the carbonyl form and the hydrate ($K_{1,2} = 1.246$ at 20 °C).[1]

$$CH_3CHO + H_2O \rightleftarrows CH_3CH(OH)_2 \qquad (1, 2)$$

The rate constant of hydration k_1 has been reported to be 9.0×10^{-3} s^{-1} at 25 °C. The establishment of the equilibrium is also proton and base catalyzed ($k(H^+) = 930$ dm^3 mol^{-1} s^{-1}, $k(OH^-) = 8 \times 10^4$ dm^3 mol^{-1} s^{-1}).[2]

Hydroxyl radicals and H atoms are generated by the radiolysis of N_2O-saturated water (reactions 3 and 4). Their radiation-chemical yields (G values) are $G(OH) = 0.57$ μmol J^{-1} and $G(H) = 0.06$ μmol J^{-1}. The radicals OH and H react with acetaldehyde and its hydrate by abstracting carbon-bound H atoms (e.g., reactions 5–8).

$$H_2O \xrightarrow{\text{ionizing radiation}} {}^{\bullet}OH, e^-_{aq}, H^{\bullet}, H^+, H_2O_2, H_2 \qquad (3)$$

$$e^-_{aq} + N_2O \rightarrow {}^{\bullet}OH + N_2 + OH^- \qquad (4)$$

$$^{\bullet}OH + CH_3CHO \rightarrow CH_3C^{\bullet}O\ (\mathbf{1}) + H_2O \qquad (5)$$

$$^{\bullet}OH + CH_3CH(OH)_2 \rightarrow CH_3C^{\bullet}(OH)_2\ (\mathbf{2}) + H_2O \qquad (6)$$

$$^{\bullet}OH + CH_3CHO \rightarrow {}^{\bullet}CH_2CHO\ (\mathbf{3}) + H_2O \qquad (7)$$

$$^{\bullet}OH + CH_3CH(OH)_2 \rightarrow {}^{\bullet}CH_2CH(OH)_2\ (\mathbf{4}) + H_2O \qquad (8)$$

It will be shown that the acetyl radical **1** and its hydrated form **2** can be distinguished by their different redox properties. The acetyl radical **1** is in equilibrium with its hydrated form **2** as is the parent compound acetaldehyde (reactions 9 and 10).

$$CH_3C^{\bullet}O\ (\mathbf{1}) + H_2O \rightleftarrows CH_3C^{\bullet}(OH)_2\ (\mathbf{2}) \qquad (9/10)$$

(1) Kurz, J. L. *J. Am. Chem. Soc.* **1967**, *89*, 3524.
(2) Kurz, J. L.; Coburn, J. I. *J. Am. Chem. Soc.* **1967**, *89*, 3528.

0002-7863/88/1510-5698$01.50/0